Versatile Sample-to-Answer Platform for Rapid, On-site Detection of E. coli DH5α Strain and Occurrence of Antimicrobial Resistance

1. Introduction

Bacterial infections present a significant risk to worldwide health. Annually, illnesses such as meningitis, gastroenteritis, pneumonia, and urinary tract infections resulting from bacteria remain a leading cause of multiple fatalities on a global scale. Timely recognition of the specific bacterial strain accountable for disease prevention is crucial in avoiding complications stemming from disease spread. It proves beneficial in devising an efficient treatment regimen for patient management. One of the leading concerns today is food poisoning, caused by foodborne pathogens, mainly Salmonella, Escherichia coli, Cholera, and other species. *Escherichia Coli (E. Coli)* is the most known pathogen among different species for food-related issues[1]. It is a rod-shaped gram-negative bacterium typically found in human and animal intestines and warm-blooded organisms. It can contaminate the food quickly and multiply rapidly in the surrounding, severely harming individuals.[2] It causes various bacterial infections, including urinary tract infections, diarrheal, and respiratory infections.

According to WHO data, 600 million people are getting sick, and 33 million die due to poor sanitation and contaminated food.[3,4] The ratio of the severity of death is higher in the children of the age group of 5 years. Due to poor sanitation and limited access to centralized diagnosis and treatment labs, bacterial infection is particularly acute in underdeveloped and underprivileged regions of developed nations. Bacterial infection-related mortalities have been on an exponential rise in the recent years.[5–7] The situation is worsened with growing antimicrobial-resistant bacteria, especially in developing countries. Therefore, appropriate treatment of antibiotics is essential in reducing the fatality and severity of the disease in a patient.[8,9] Although there are advancements in detecting pathogenic bacteria and microbial resistance, there are many limitations, including poor accuracy, time-consuming methods, and manual interventions affecting treating bacterial infections at an early stage.[10–12]

Common antibiotics can be used to treat E. coli infections. Still, some strains of this bacteria have become resistant to them, which can result in extended recovery durations or even death.[13,14] Drug-resistant bacteria are progressively emerging as one of the significant public health issues as the development of new antibiotics is sluggish and difficult. Alexander Flemings, a physics scientist, accidentally discovered the first antibiotic, penicillin, to treat bacterial infection. That simple discovery saved millions of lives over decades.[15,16] Several

antibiotics have been prepared and discovered over the years. However, with time, these microorganisms become resistant to the drugs.[17,18] Antimicrobial resistance arises when microbes do not have a more extended response to the medicine, making the infection harder to treat.

Therefore, with minimalistic symptoms and the onset of infection, it is crucial to identify the micro-organism and the effective antibiotic against it. An antimicrobial resistance (AMR) test is often conducted, and the conventional approach is adapted to determine the effectiveness of antibiotics in curing the infection. [19,20] Generally, AMR shows the type and quantity of antibiotic working against the micro-organism. Lately, clinicians have recommended AMR significantly to prevent antibiotic toxicity in the patient.[21,22]

Continuous antibiotic exposure causes a mutation in the microbial gene, leading to resistance in the strain. Therefore, knowing antibiotic effect, dosage, and duration before use is essential. Antibiotic susceptibility testing (AST) helps identify the pathogen and the most effective antibiotic against it.[23,24] AST provides information on selecting antibiotics and evaluates the minimum inhibitory concentration. It detects both phenotype and genotype resistance. Genotype is classified based on the presence or absence of a resistant gene, and phenotype is found without the gene mutation.[25–27] Although advancements in detecting pathogenic bacteria and microbial resistance exist, poor accuracy, time-consuming methods, and manual interventions affect the overall treatment of bacterial infections at an early stage.[28,29]

Traditional methods like cell culture, PCR, and Enzyme-Linked Immunosorbent Assay (ELISA) are molecular and immunoassay-based diagnostic tools deployed for specific detection of pathogenic bacteria.[30,31] However, PCR leads to nonspecific amplification and the generation of false positive data. Other techniques, like disk diffusion, are available, which is the gold standard for AST, is quick to execute, can identify many antibiotics in a single test, and allows for a wide range of antibiotic choices. Still, it takes time and cannot provide MIC values.[32,33] Another method is broth dilution, which is straightforward, legitimate, and easily accessible but demands more supplies of reagents and introduces more excellent room for error.[34]

Moreover, 4-5 days are reportedly needed resistance to detect the bacteria and its resistance to clinically detect the bacteria and its resistance clinically. Owing to this, the infection increases, or sometimes even delays could be fatal. Hence, the need of the hour is for novel technologies to develop a Rapid Diagnostic Test (RDT) to detect the causal microorganism for bacterial

infection to identify the causative bacteria.[35] Hence, developing rapid techniques for measuring antibiotic effectiveness will improve global health and decrease mortality. A quick, sensitive, miniaturized device could address the existing limitations.

Furthermore, the bulky instrumentation, costly diagnosis, and unavailability of point-of-care facilities lead to delays in treatment. Hence, there is a critical need for compatible diagnostic devices to detect bacteria and their growth.[36] The conventional diagnostics techniques to detect the causal organism for bacterial infection are complete blood count and measuring blood biomarkers levels.[37] However, the utility of diagnosing or predicting bacterial infections as part of routine clinical practice has yet to be established. Therefore, the gold standard assay for detecting bacteria is based on a time-intensive bacterial culture. [38,39]

Early detection of bacterial infection and prevention of antimicrobial resistance propose a new perspective for novel, inexpensive, sensitive, and rapid device development. Hence, the development in the field of microfluidics has built a paradigm shift in the detection of bacteria and high-precision laboratory equipment.[40] Microfluidic reduces the number of steps required for an experiment by combining them into one step.[41,42] It also increases portability, reduces the requirement of sample and reagent, improves automation, decreases power consumption, and provides high throughput detection.[43] In the Lab-On-a-Chip (LOC) technologies framework, microfluidics has started to play a significant role in the analytical examination of biological and chemical samples in a single miniaturized device. These devices are excellent for POC applications due to their intrinsic qualities.[44] Due to its versatile application, microfluidic devices are more effective in detecting pathogens and antimicrobial resistance early than conventional methods.[45] The microfluidic device integrated with the electrochemical system further increases the sensitivity and improves the detection efficacy.[46,47]

The present study has developed a rapid, sensitive, miniaturized electrochemical device for simultaneous culturing, detection, and multiplexed antibiotic susceptibility testing.[48] Here, E. coli was used as a model microbe for testing the device. The three-electrode system was fabricated using a screen-printing technique modified with graphitized mesoporous carbon (GMC), which was used as a working electrode for testing. Ag/Agcl paste modified electrode as a reference electrode and carbon ink as a counter electrode. GMC is a high surface area carbon material that sensitively detects E. coli. The developed sensor could detect bacteria, culturing, and antibiotic susceptibility testing (AST). The repeatability, sensitivity, and stability

testing were studied for the designed device. The specificity study of the device for detecting bacteria and particular antibiotics toward E. coli was validated using different pathogens like Streptococcus Pneumonia, Pseudomonas aeruginosa, and Shewanella Putrefacient bacteria. For the AST, various antibiotics were screened by checking the minimum inhibitory zone, and the one with a more significant inhibition zone was selected for susceptibility testing. The different antibiotic concentrations were prepared, and efficacy was checked using the electrochemical cyclic voltammetry (CV) method. The fundamental sample analysis used pure mango juice, artificial urine, and water samples. The obtained results were further validated with the conventional broth dilution method. To the extent feasible, this is a benchmarking prototype study that has yet to be explored so far. The strategy with further optimizations can also be used for other micro-organisms in real time. The detailed schematic is shown in Fig 1.

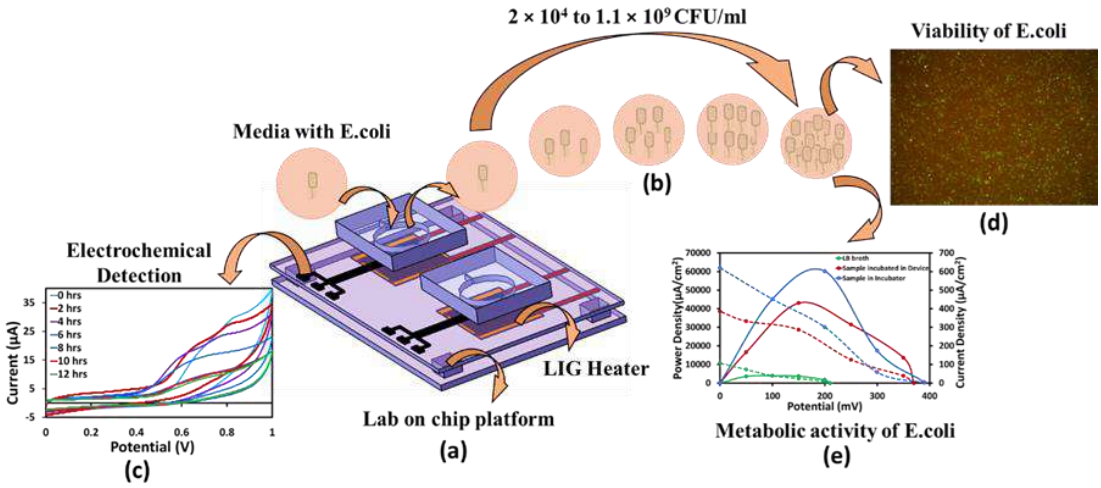

Fig 1. Schematic describing the overview of the presented work, showing (a) schematic of a microfluidics device integrated with screen-printed electrodes and a LIG heater, (b) on-chip bacterial incubation, (c) simultaneous electrochemical detection of bacteria, (d) confirmation of bacterial viability through fluorescence imaging (e) validation of metabolic activity by using the cultured bacteria for a microbial fuel cell.

2. Objectives

The proposed project aims to develop a Versatile Sample-to-Answer Platform for Rapid On-site detection of E. coli DH5α bacteria and its Antimicrobial Resistance strain (AMR). The following are the primary objectives of the project.

1) Design, fabrication, and characterization of electrodes and microfluidic channels for electrochemical sensing.

2) Immobilizing biorecognition elements over the electrode surface for selective, sensitive detection of different pathogens.
3) Simultaneous Detection of Pathogens and AMR Genes.
4) On-chip testing of real/clinical samples.
5) Development of fully portable IoT enables platform for real-time, continuous detection of bacterial infection and antimicrobial-resistant strains.

3. Material and Methods

3.1 Materials

Luria broth and Luria agar were procured from Thermo Fisher Scientific, India. Potassium chloride, Carbon ink, glass slide (75×50 mm), Ammonium phosphate, sodium sulfate, Sodium phosphate monobasic dehydrate (NaH2PO4. 2H2O), and Sodium phosphate dibasic dehydrate (Na2HPO4. H2O), ammonium diphosphate, magnesium chloride, calcium chloride, creatinine, and urea were purchased from Sigma Aldrich, limited. E. coli culture was acquired from the Biological Science Department, BITS Pilani Hyderabad campus. Clavam 625 (Amoxicillin and Clavulanic acid), Zenflox 200 (Ofloxacin), Monocef-O 200 (Cefpodoxime), Cifran 500 (Ciprofloxacin), and Azee-500 (Azithromycin) were purchased from a local medical store. Polydimethoxysilnae (PDMS) was purchased from Delta Silicon, Mumbai, India. A CO_2 laser (VLS 3.20) was procured from Universal Laser Systems, USA, and PMMA (polymethylmethacrylate) and PVC (polyvinyl chloride) sheets were

purchased from Amazon.

3.2 Methodology

3.2.1 Fabrication of Three-Electrode System for Electrochemical Detection

The screen-printing process was utilized to prepare a three-electrode system. The design of the requisite dimension was first drawn using solid work software. A Polyvinyl chloride (PVC) sheet was stuck to the glass side (75×50 mm), and the laser was scribed over the PVC sheet to prepare the mask. The carbon ink was laid down over the obtained mask with the help of a squeeze and kept in the oven for 30 minutes. The PVC sheet was removed after drying, and the screen-printed electrodes were obtained [49]. Fig 2 depicts a detailed schematic of the fabrication process.

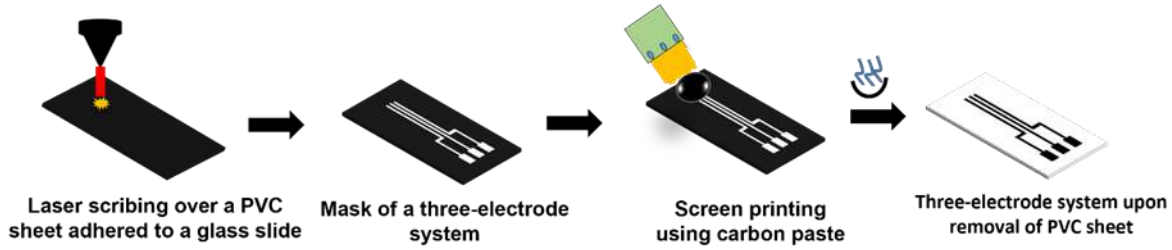

Fig 2. A schematic for the development of a three-electrode system using the screen-printing technique.

3.2.2 Design and fabrication of Microfluidic channel for bacteria culturing

A mold of 2×1.4×17 mm^3 dimension was prepared on the acrylic sheet to develop the microfluidic device. To create a PDMS mixture, epoxy and curing agent were mixed in a 10:1 ratio and degassed for 30 minutes to remove the oxygen bubble. Following this, PDMS was run over the mold and baked for an hour at 70°C. Post-curing, the reservoir was cut from the mold and bonded over the three-electrode system using the plasma bonding method. The Final electrochemical devices is shown in fig 3.

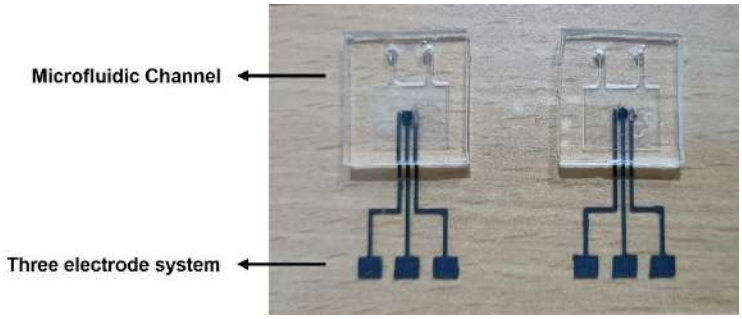

Fig 3. A microfluidic device integrated with a three-electrode system

Initially, an aluminum-based heating block was utilized for the incubation of bacteria. An aluminum block was assembled with a heating sensor and temperature controller by fabricating a miniaturized 3D-printed shell. On the one end, the heater, while on the other end, the temperature sensor was fixed inside the fabricated shell. The temperature controller is tuned to supply the appropriate temperature, i.e., 37°C, and programmed in a manner to control the required temperature properly. Hence, upon receiving the system's feedback, the installed temperature controller turns off the heater. The integrated setup is shown in Fig 4.

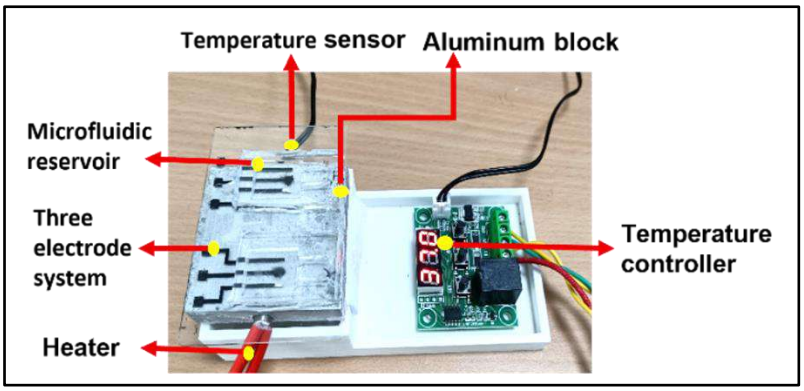

Fig 4. The microfluidic device is integrated with screen-printed electrodes, an aluminum block, and a thermal management system (Heater and temperature sensor) supported by the controller.

3.3 Bacterial Incubation Method

In addition to this, an in-house, low-cost LIG heater was fabricated for bacterial incubation and compared with a commercially available aluminum-based heating block. For the fabrication, a polyamide sheet of the required dimension of 25×25 mm was initially pasted onto a glass slide surface using double-sided tape. The CO_2 laser (VLS 3.60) was exposed on the polyimide sheet with power and speed of 6.5% and 4.5% to obtain Laser-induced graphene.[51] After engraving, the obtained thickness was 50 µm. The electrical contacts were provided on the fabricated LIG film using copper tape and silver ink. The thermal factor was calibrated earlier by varying the potential and noting the temperature. A temperature of 37^0C was maintained by applying a potential of 2.5 V. A thermal camera was used to keep track of the achieved temperature. Figure 5 (a) shows the step for fabricating the LIG heater, and (b) shows the temperature of the LIG heater, which was maintained at 37 ± 1^0C.

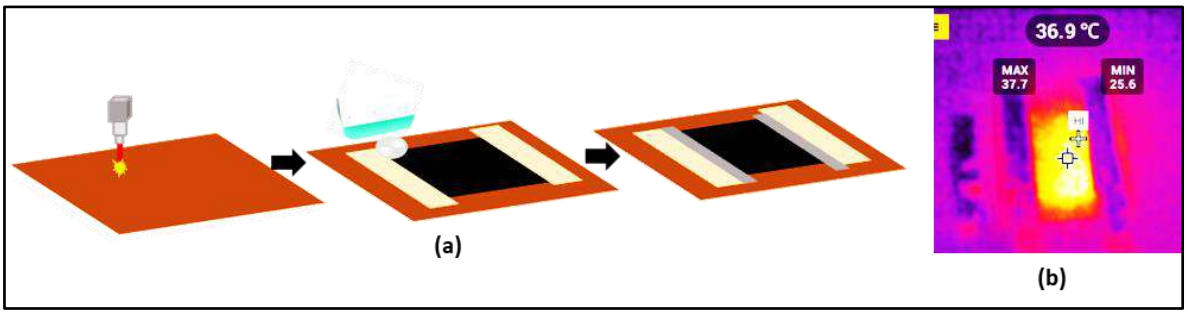

Fig 5. (a) Fabrication steps for LIG heater (b) The image of the Laser-induced graphene heater captured by a thermal camera after heating while providing a voltage of 2.5V.

The microfluidic reservoir was mounted on the screen-printed electrode using plasma bonding, and a laser-induced graphene heater was stuck to the back of the printed electrodes. The image of the final developed microfluidic device integrated with the LIG (Laser-induced graphene) heater is shown in Fig 6.

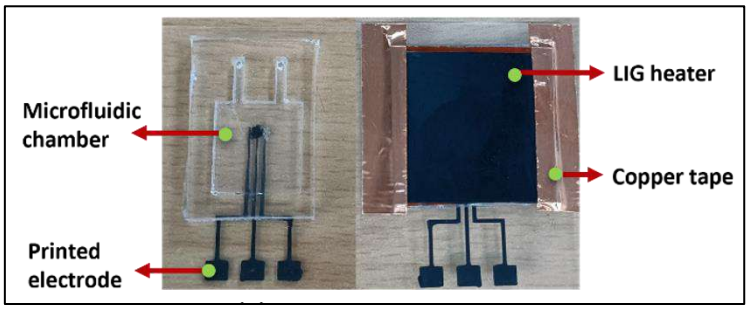

Fig 6. A miniaturized device integrated with a LIG heater provides temperature, and copper tape provides electrical contacts connected to the voltage regulator.

Furthermore, an inkjet-printed silver microheater was developed to enhance flexibility and reduce power consumption. Silver ink was chosen for its low cost, excellent conductivity, and easy deposition. Polyimide was used as the insulating substrate due to its low thermal conductivity and ease of fabrication. The microheater's conductive traces were printed on a 0.25 mm thick polyimide sheet using a Voltera V-One inkjet printer. After printing, the patterns were dried at 65°C for 15 minutes. The fabricated microheater was used for heating characterization and bacterial incubation. The fabricated microheater is shown in Fig 7.

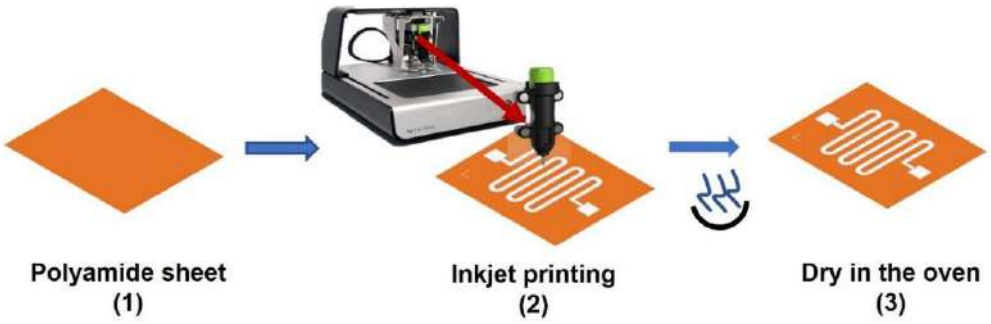

Fig 7. Stepwise fabrication flow for the microheater

3.4 Bacterial sample preparation

E. coli $DH_5\alpha$ strain bacteria was used in this experiment. For the Cultural preparation, 200 µl of E. coli. During the trial, 200 µl of *E. coli* $DH_5\alpha$ culture was inoculated into a 20 mL LB broth and incubated (37^{o} C, using a continuous shaker at 180 Rotation Per minute) for about 36 hours. Eventually, the optical density was determined by a smart digital photo colorimeter.

After that, the recently cultured microbial sample was diffused and submerged in a pH seven phosphate buffer solution (PBS).[52] Finally, the microbial cultured sample was diluted in a different concentration from 0.336×10^{7} CFU mL^{-1} to 40×10^{7} CFU mL^{-1}. CFU mL^{-1} is the most used unit for measuring *E. coli* bacterial concentration. A colony-forming unit is referred to as a CFU. The current changes on the surface of the electrode were recorded as a function of concentration.

The serial dilution and plate count are represented diagrammatically in Fig 7. Determining the unknown quantity of a sample (number of bacterial colonies, organism, bacterium, etc.) is the primary goal of the serial dilution method. A series of dilutions (10^{8}–10^{12}) were created from the original inoculum to count the number of bacteria in the solution using a plating procedure. There were six agar plates made. Each diluted tube's sample was speeded 100 µl over the agar plate. The plates were incubated at 37^{0}C for 12 hours, and colonies were manually counted using just the naked eye. Between 30 and 300 colonies should be measured in a sample. Colonies on a plate with more than 300 CFU will swarm together and overlap.[49]

Number of microorganisms (CFU mL^{-1}) = (number of bacterial colonies x total dilution factor) / volume of the cultivated plate in mL is a formula for calculating the CFU.

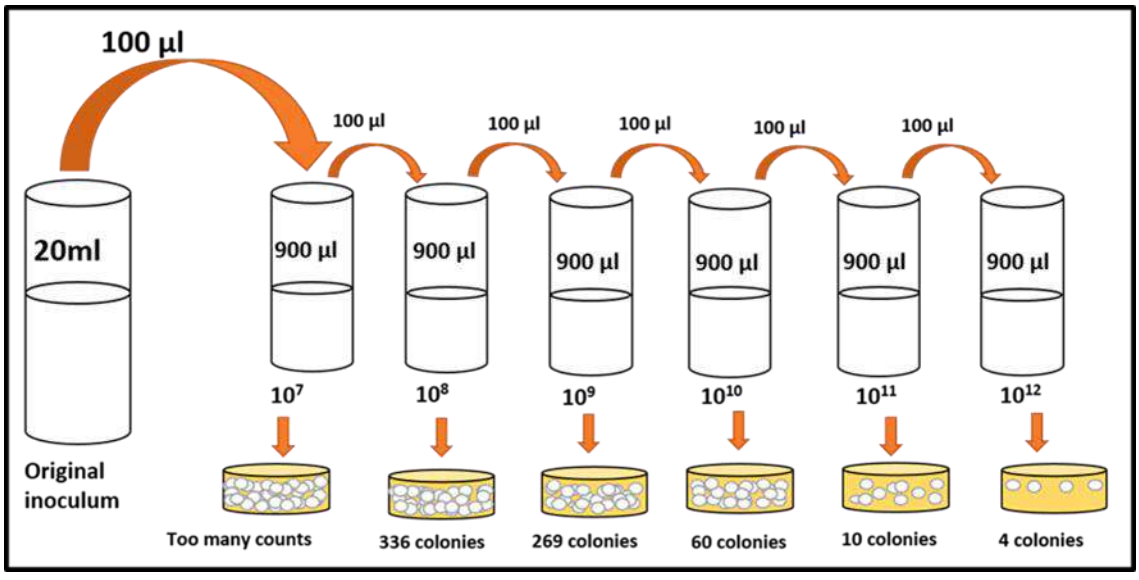

Fig 9. Schematic of serial dilution method and plate count

3.5 Multiplexed Device for On-Chip Bacterial Incubation and Detection

The portable device was designed for bacterial incubation, detection, and antibiotic susceptibility testing. It featured a fully integrated system with a bacteria-on-chip setup for culturing bacteria. A flexible heater maintained the incubation temperature at 37°C, regulated by a voltage controller to ensure consistent heating. A temperature controller was also included to manage the 37°C requirement precisely. The entire system was powered by a battery, ensuring portability and convenience. All components are securely enclosed in a 3D-printed casing with dimensions of 100 mm × 100 mm × 20 mm (length × width × height), fabricated using a layer-by-layer fused deposition process.

An on/off push button was connected to the battery and temperature controller. When the button was pressed, the battery powered a buck-boost converter, providing 1.5 V to the heater, maintaining the required 37°C. This temperature was monitored and controlled by the temperature controller. The heat generated by the flexible heater was transferred to the bacteria-on-chip, facilitating bacterial incubation. Electrodes on the chip were connected to a Potentiostat through a card edge connector to monitor the electrochemical response during the process. The complete device is illustrated in Fig 10.

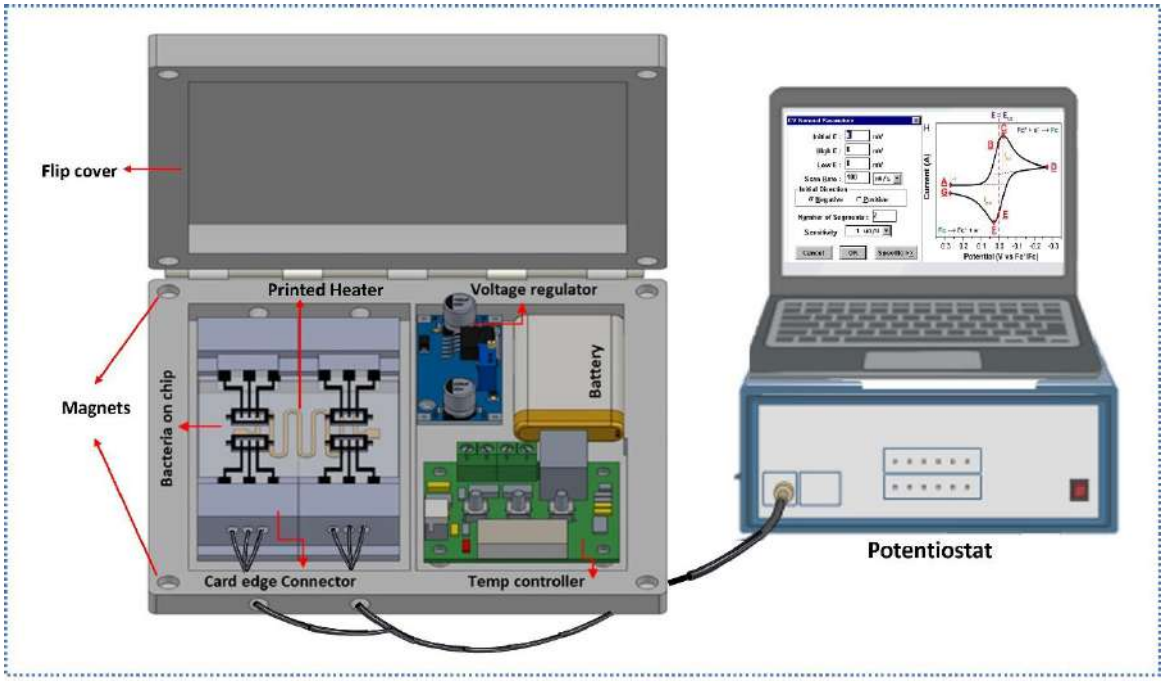

Fig 10. Multiplexed biosensing platform for on-chip bacterial incubation, detection & antibiotic susceptibility testing.

3.6 Electrochemical detection of bacteria

A Potentiostat (Origaflex 500 from Origalys, France) was employed for the electroanalytical measurement. A screen-printed three-electrode system, comprising a GMC electrode, Ag/AgCl as a reference electrode, and carbon ink as a counter electrode, was used throughout the electrochemical analysis. GMC has a large surface area, higher void space, and good heat resistivity, which increases its activity manifold in performing functions. For measurement, sodium phosphate monobasic dihydrate (1.171 g) and sodium phosphate dibasic dehydrate (2.171 g) of concentration 0.1 M were combined to make phosphate-buffered saline (PBS). The pH of the electrolyte was altered to 7.4 using 0.2 M sodium hydroxide.

3.7 Electrochemical Characterization of Electrodes

The electrochemical behavior of the fabricated microfluidic device integrated with screen-printed electrodes was checked by performing cyclic voltammetry. 5 mM of the $K_3Fe(CN)_6$ mixed with 1 mM potassium chloride was drop-casted onto the electrodes to understand the transfer rate. [50] The observed results highlight the appropriate transfer of electrons with a clear indication of oxidation and reduction peaks within the potential range of -0.7 V to +0.7 V, which was achieved by performing cyclic voltammetry at a scan rate of 50 mV/s, as shown in Fig 8 (a). Additionally, the electrodes were evaluated for plain LB media between 0 and 1, and a correct media peak was found at a potential close to 0.8 V, as shown in Fig 8 (b).

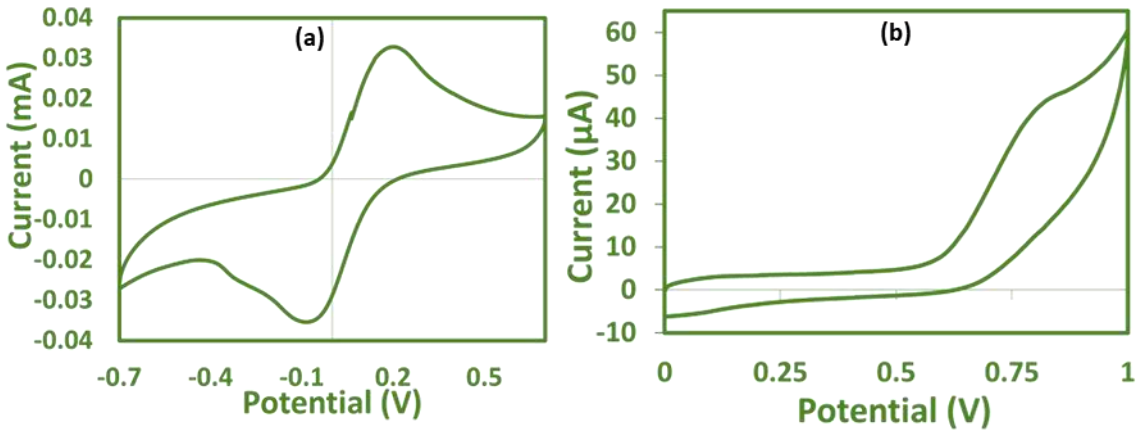

Fig 8. Cyclic voltammograms showing (a) potassium ferricyanide at potentials between -0.7 and +0.7 and (b) plain LB media without bacteria at potentials between 0 and 1.

3.8 Effect of antibiotic on the E. coli

Electrochemical analysis was used to determine the effect of antibiotics on bacterial growth. A Potentiostat (CHI 1030E) was utilized to record the electrochemical response. A three-

electrode setup was employed, with a reference electrode of Ag/AgCl, a working electrode of GMC, and a counter electrode of plan carbon ink.

3.9 Real-Sample Analysis

Juices and related foods are frequently linked to outbreaks of foodborne illness.[41] From the grocer, mango juice was purchased. The mango juice's pH was raised to 6.94. Colonies of E. coli were removed from the plate and diluted in mango juice. The microfluidic apparatus received the prepared sample by injection. The produced samples were then subjected to electrochemical detection.

For antibiotic susceptibility testing, synthetic urine and tap water. The synthetic urine was prepared by adding all dried components to sterile water. Normal urine is a mixture of organic compounds such as urea, creatinine, and uric acid and inorganic substances like ammonia, sulfates, chloride, and phosphates. The composition of prepared synthetic urine is mentioned in Table 1.

Table 1. The composition of synthetic urine

Components	**Quantity (mg/L)**
Potassium Chloride (KCL)	2000
Sodium Sulfate (Na_2SO_4)	2000
Ammonium Phosphate ($(NH_4)_3PO_4$)	850
Ammonium Diphosphate ($(NH_4)_32PO_4$)	850
Calcium Chloride ($CaCl_2$)	250
Magnesium Chloride ($MgCl_2$)	500
Urea (CH_4N_2O)	600
Creatinine ($C_4H_7N_3O$)	50

4. Result & Discussion

4.1 Microscopic study of Graphitised mesoporous carbon-modified electrode

The GMC-modified electrode's FESEM (field emission scanning electron microscopy) pictures are shown in Fig 11. The FESEM analysis assesses the physicochemical characterization of

various nanomaterials and determines the components' quantitative value. The photograph shows that mesoporous carbon was evenly distributed across the electrode surface.

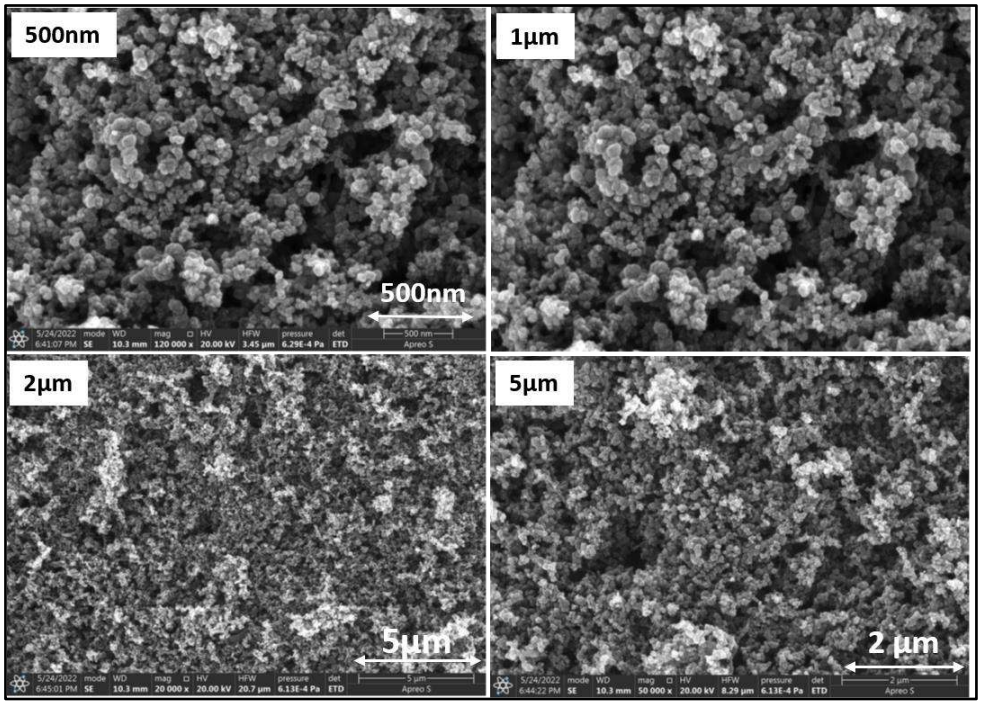

Fig 11. SEM images of GMC modified electrode with different magnification.

4.2 Bacteria Growth Kinetic Study

A syringe was used to transport the sample within the microfluidic reservoir. Before the trial, the pool was cleaned in 0.1 M PBS (pH 7.4) for 15 minutes. The prepared bacterial inoculated sample was injected into the microfluidic device, and temperature (37^0C) was provided using the thermostat. To study how bacterial growth relates to time, an electrochemical measurement was directed by CV for a period of 36 hours at intervals of 4 hours, as shown in Fig 12. A voltammogram for E. coli samples taken at various time intervals is shown in Figure 13 (a). Similarly, the samples that were incubated conventionally also underwent CV, and their voltammograms were compared to those of the samples in the microfluidic device. 13 (b) represents the cyclic voltammetric curve for an example of bacteria cultivated in the conventional incubator. The bacteria concentration would increase in the microfluidic device with time and a steady temperature supply. The peak current values in the graph progressively decline over time. As time goes on, the peak current steadily declines, which must be made possible by a rise in the bacterial content in LB media. In cyclic voltammetry, a decrease in peak current is associated with increased bacterial incubation.

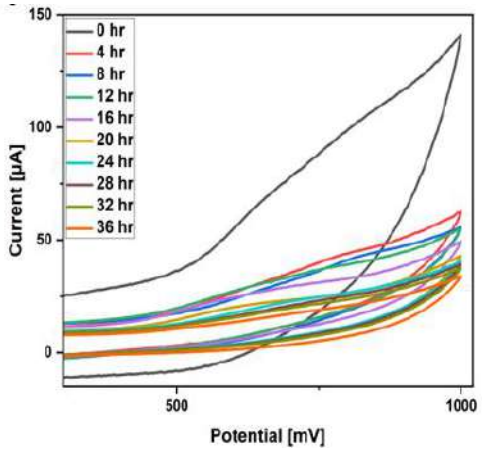

Fig 12. The electrochemical response to growth study was conducted for 36 hours, and the answer was recorded at 4 h.

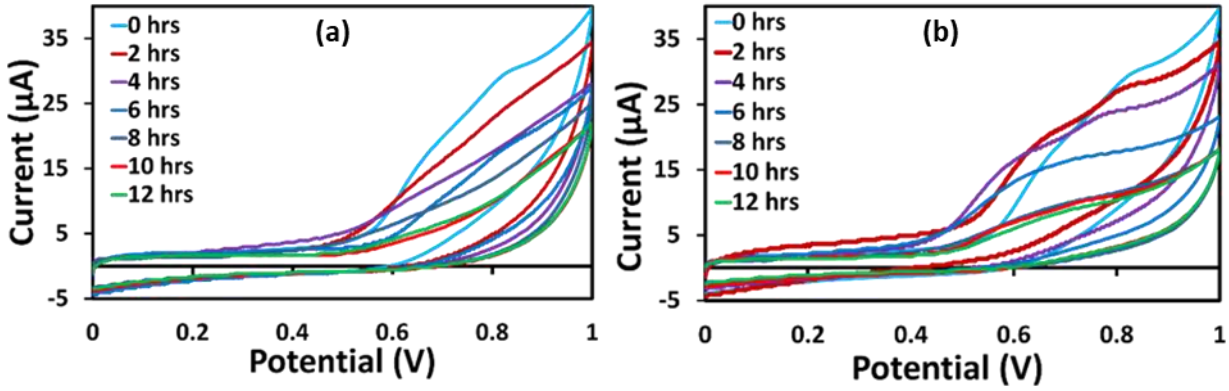

Fig 13 (a) Conventional incubator and (b) microfluidic device were used to record cyclic voltammograms for 12 hours at various bacterial concentrations ranging from 2×10^4 to 1.1×10^9 CFU/ml.

The conventionally incubated sample and the microfluidic device were compared using a comparison plot (Fig 14(b)), where a linear fit was found with a regression coefficient of 0.99. This implies that bacterial culture on a microfluidic device is just as proficient as bacterial culture in a traditional incubator.

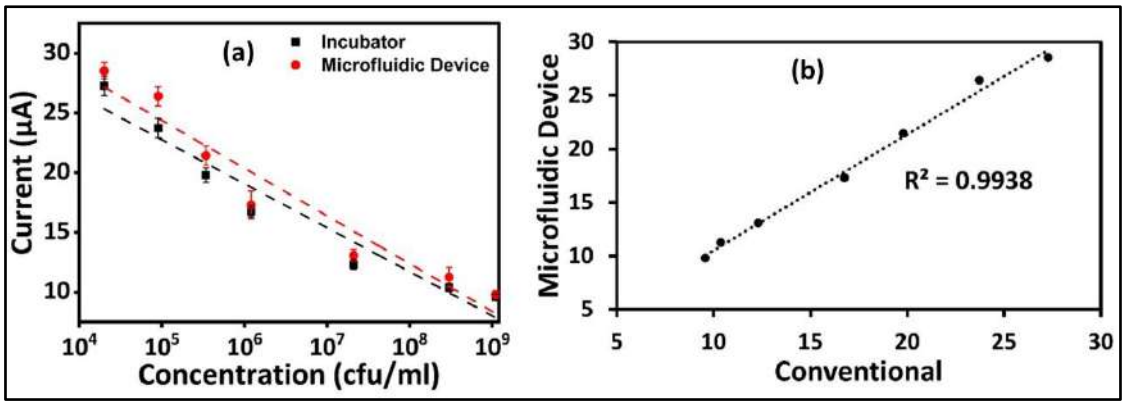

Fig 14 (a) shows calibration plots for samples in a traditional incubator and a microfluidic device (standard deviations are calculated from three experiment sets) using cyclic voltammogram data. The comparative action of the currents from the conventional and microfluidic approaches is shown in (b).

4.3 Concentration Study of Bacteria

E. coli was prepared in PBS buffer (pH 7.44 and an Optical density score of 1.12) and inserted into the microfluidic device to detect the bacteria in different concentrations. The attention of bacteria varied from 0.336×10^{12} to 40×10^{12} CFU mL-1, and the cyclic voltammetry was utilized to measure the peak current in the potential range +1 to -1 V and a scan rate of 50 mV s-1. The chosen range was sensitive to the GMC electrode; there was no chance of detecting bacteria below it, and electrode saturation was seen. The CV answers are displayed in Fig 15 (A). As the E. coli bacterial concentration rises by ex-situ addition, the peak current also increases. The blue line in Fig 15 (A), which has the lowest current value, had the lowest concentration. The related linear plot between the peak current values (A) and the concentration (CFU mL^{-1}) is shown in Fig 15 (B). The calibration curve of Epa vs. Conc was used to calculate the correlation coefficient value. R^2 = 0.997 was recorded as the value. This represents the quantity of active sites that are present on the electrode. The limits of detection (LoD) and quantification (LoQ) were calculated from the minor concentration triplicated experiment using LoD=3.3/slope, LoQ=10/slope, and standard deviation represented by. According to calculations, the device's LoD and LoQ are 0.35 and 1.05 CFU mL^{-1}, respectively.

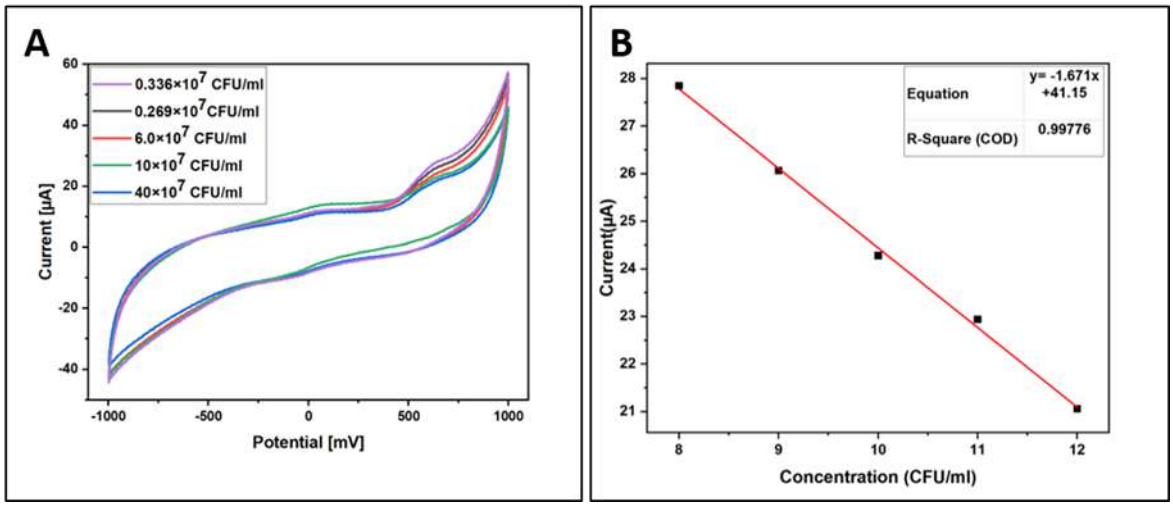

Fig 15. A) Concentration effect of E. Coli and its respective B) Calibration plot

4.4 Viability of live/dead bacterial cells

Fluorescent imaging was performed to determine the viability of the bacteria that was still alive or died after the culturing. The STYTO 9 and Propidium iodide stains were used to check the viability of the bacteria cell. The bacteria sample from a conventional incubator and microfluidic device was mixed with stains and kept dark for 15 minutes. After that, the sample was checked using a fluorescence microscope. It was realized that a relatively tiny number of dead bacterial cells were there, and an active population of bacteria after 12 hours was present. Fig 16 (a) and (b) show bacterial growth in conventionally cultured samples, whereas Fig 16 (c) and (d) highlight a sample grown in a microfluidic device. It was observed that the presence of dead bacteria was greater in a sample cultured in an incubator than in the microfluidic device. Hence, the actual growth of the bacteria was seen in the microfluidic channel, which was evident from the fluorescent images, and it is highly dependable to detect this development using screen-printed electrodes [50].

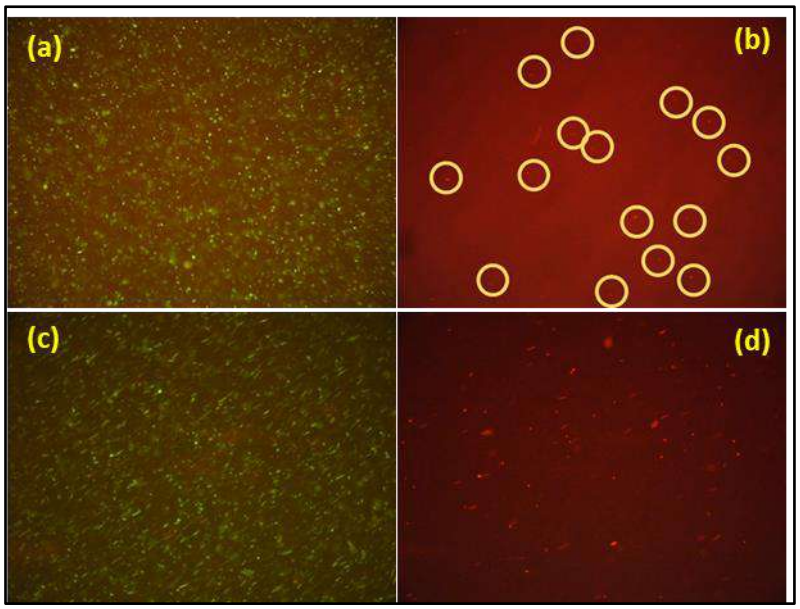

Fig 16. Fluorescent pictures demonstrate the viability of bacteria after a 12-hour culture (a) living bacteria in a traditional incubator, (b) dead bacteria in a traditional method, (c) live bacteria culture in a microfluidic device, d) dead microorganisms in a microfluidic device.

4.5 Metabolic Activity of the bacterial cell

In the real-time applications of the developed platform, metabolic activity is quite crucial. To realize its application in the real world, a microbial fuel cell (MFC) was used to understand the metabolic activity of the grown bacteria**.** Few publications have previously discussed using bacteria as a source of fuel for a fuel cell. [53] The impact of cultured bacteria on the achieved power density microbial fuel cell was fabricated by a 3D-printed paper-based approach, as published in one of our earlier research projects.[54] Carbon paste and silver nano ink were used to manufacture an anode and a cathode, respectively. The cathode was modified with MnO_2 nanoparticles to improve it further. After manufacture, silver ink was applied to the electrodes to create the electrical connections. The efficiency performance of microbial fuel cells was studied by utilizing three distinct samples: traditional setup, plain LB media, and microfluidic device, was taken into consideration. When a stable open circuit voltage (OCV) was reached, 0.1 ml of LB broth was drop-casted on the anode, and the values were then recorded. For the remaining two cases, the same procedure was followed. After stabilization, the polarization curves were plotted to achieve the maximum power and current density in the three scenarios (Fig 17).

A maximum power density of 4 W/cm^2 was reported for plain LB media. However, the sample, including bacteria, produced more power. The power density of the sample incubated in a

microfluidic device was determined to be 43 W/cm^2, while the power density of the bacteria cultivated in a conventional setup yielded 61 W/cm^2. According to Fig 14, more dead bacterial cells were present in the sample cultivated in a microfluidic device than in the conventionally cultured bacteria, which is thought to be the cause of the sample's lower power density. However, these power density numbers demonstrate that the bacteria in the microfluidic device have grown successfully since their metabolism has generated a respectable level of power density in contrast to other MFCs on the market.[55] This shows that the metabolic activity of the bacteria grown in the microfluidic device was comparable to the sample grown in an ordinary incubator.

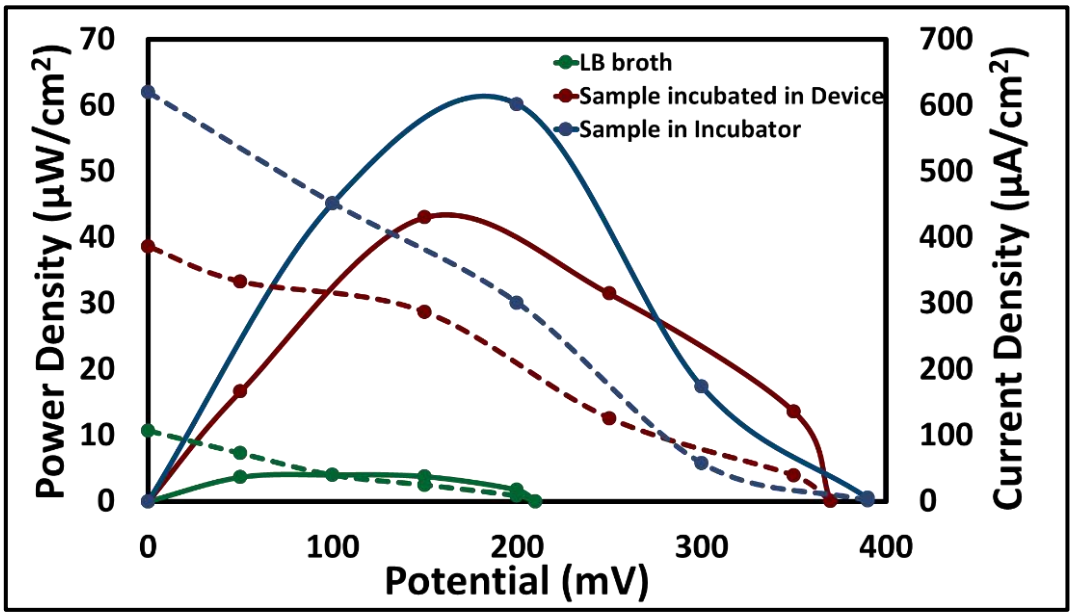

Fig 17. Polarization curves for power density and current density for bacteria grown on plain LB media, in an incubator, and in a microfluidic device.

5. Development of a portable incubator cum detector for bacteria growth

The packaging was designed and manufactured using 3D printing technology to integrate the microfluidic chip with an in-house fabricated heater and the detection unit. The voltage is regulated using a commercially available DC-DC buck booster for powering the heater and the hand-held portable Potentiostat (Sensit smart; Palm Sens, Netherlands) connected to a smartphone. Fig 18 (a) and (b) show the device setup fabricated for electrochemical testing. After setting up Everything, the sample was injected into the microfluidic chip, and the heater received the necessary power to maintain the proper temperature for the bacteria's incubation. The inset of Fig 18 (c) displayed the first readings for the bacterial growth on ordinary LB media.

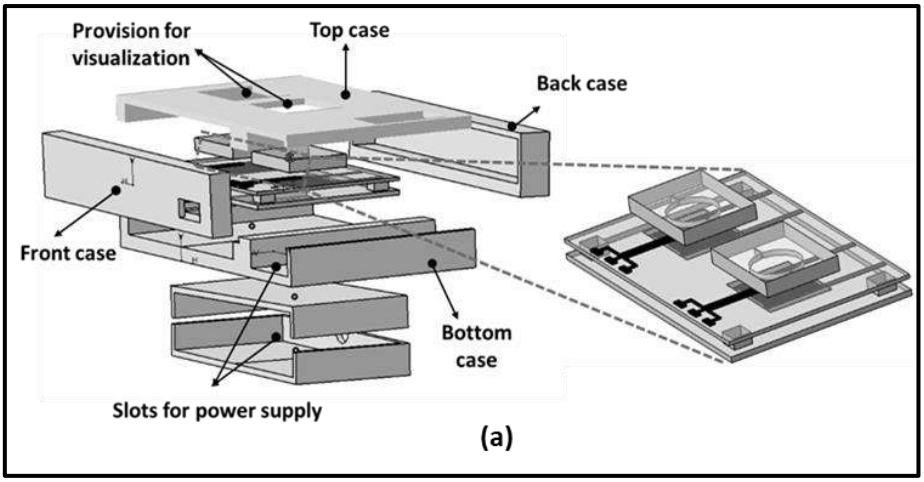

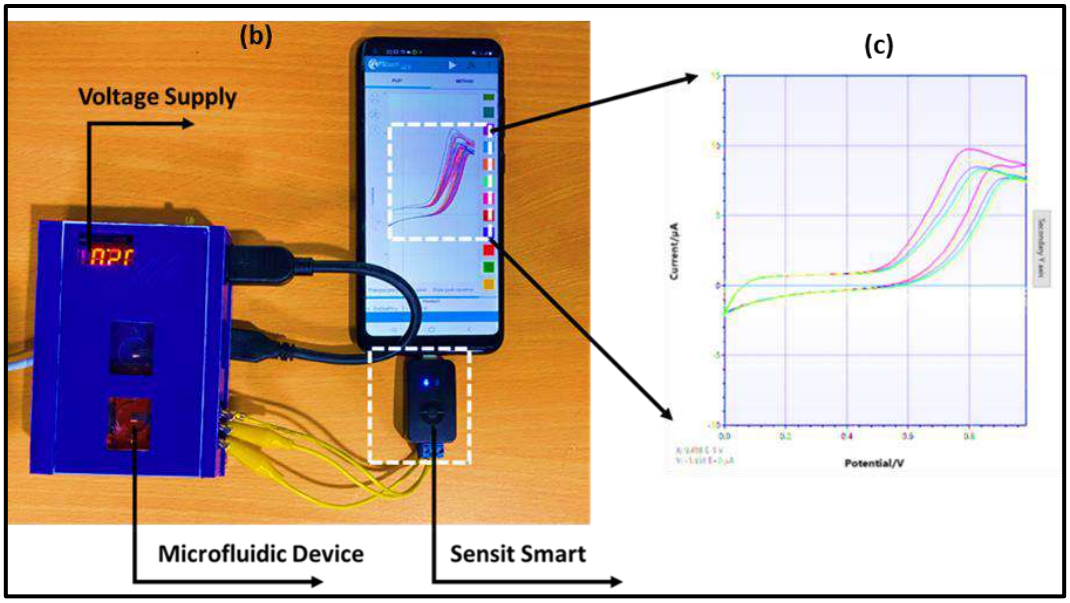

Fig 18 (a) Schematic of the portable gadget showing its various components and an integrated microfluidic device (b) A handheld device that has been realized and is connected to a portable Potentiostat. The device's dimensions are 110(l) x 85(b) x 40(h) mm. (c) The output curves for bacterial growth in the microfluidic device.

Reproducibility study

The reproducibility study was done using various devices to ensure the consistency of the electrode. The device's repeatability was evaluated from 6×10^7 CFU mL-1 of E. coli. Two devices that used electrochemical detection produced a repeatable peak current value with a relative standard deviation of 0.41% (less than 10%), as shown in Fig 18. The measured relative standard deviation values indicate the device's repeatability.

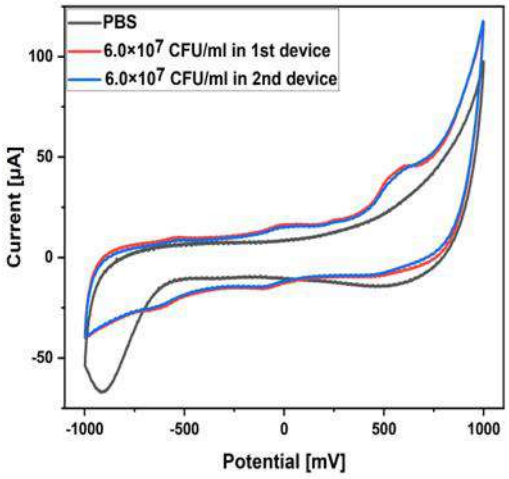

Fig 19. Reproducibility study of the two different devices

Mechanism of Action of Antibiotics

Antibiotics are medicines that fight bacterial infection by directly killing or slowing down the growth of bacteria. [56,57] They are classified into different types based on spectrum, i.e., broad and narrow-spectrum antibiotics. Based on mode of action, i.e., bactericidal and bacteriostatic, and based on chemical structure, i.e., B-lactam, aminoglycoside, chloramphenicol, glycopeptides, sulphonamide, tetracycline, macrolides, oxazolidinones, quinolones. All of them have different mechanisms to kill bacteria[58]. This antibiotic prevents the growth of bacteria by preventing the synthesis of 1) cell walls, 2) nucleic acids, 3) metabolic pathways, 4) membrane function, and 5) ATP. The details of the mechanism are represented in Fig 20. The experiments used Four antibiotics: Cefpodoxime, Ofloxacin, Amoxicillin Clavulanic acid, and Ciprofloxacin.

Cefpodoxime is the third-generation derivative of cephalosporin used to diagnose bacterial infections, including pneumonia, sinusitis, and gonorrhea. Both gram-positive and gram-negative bacteria are resistant to it. It inhibits the peptidoglycan layer of cell wall synthesis.

Ofloxacin comes under fluoroquinolone derivatives for treating respiratory, kidney, soft tissue, and urinary tract infections. It is a broad-spectrum antibiotic that blocks the enzyme DNA topoisomerase-IV and gyrase, which prevents DNA replication.

Amoxicillin and Clavulanic acid are a combination of two that help to treat antibiotic resistance. It is the broad spectrum used to treat sinusitis, lower respiratory infection, otitis media, skin infection, and urinary tract infection. It inhibits cell wall synthesis by inhibiting the beta-lactamase enzyme.

Ciprofloxacin is a broad-spectrum antibiotic that comes under second-generation fluoroquinolone derivatives. It treats urinary tract infections, pneumonia, and other skin and bone infections. Also, it inhibits the topoisomerase II and topoisomerase IV enzymes and prevents DNA replication. Fig. 3 shows a brief overview of the mechanism of antibiotic action. [59]

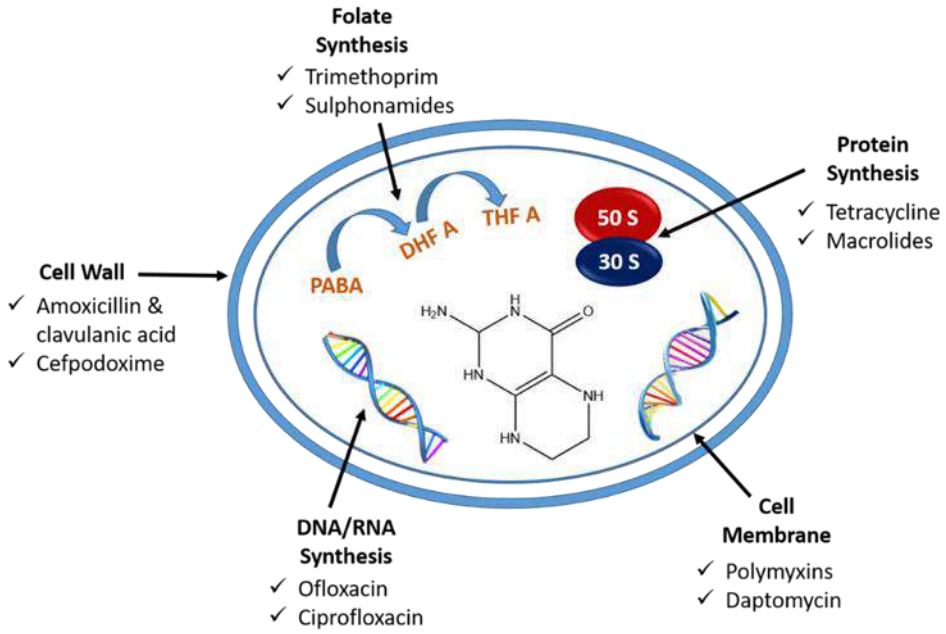

Fig 20. Schematic representation of the mechanism of action of antibacterial drugs.

Off-Chip MIC calculation

The model microorganism used was Escherichia coli (DH5α strain). An agar plate containing Luria Bertani broth (LB) was used to sustain E. coli cells. E. coli colony cells, after removing from the agar plate, were suspended in 5 mL of LB liquid media. Overnight at 37° C, the cells were cultured in the medium on a shaker at 200 rpm. After that, a fresh LB medium was used to dilute the cell suspension until it reached an optical density of 0.01 at 600 nm.[60]

The antibiotic stock solution (1 mg/ml) of Cefpodoxime, Ofloxacin, Amoxicillin, Clavulanic acid, and Ciprofloxacin was prepared in sterile water. Several concentrations, ranging from 100 to 500 g/ml, were prepared from the stock solution, and the minimal inhibitory concentration was measured using a disc diffusion approach. The LB agar media was prepared and poured into a Petri plate. After solidifying the agar gel, the bacterial culture was spread over the plate. Using sterile forceps, an antibiotic disc of Cefpodoxime, Ofloxacin, Amoxicillin, Clavulanic acid, and Ciprofloxacin was applied to the plate and incubated for 12

to 24 hours at 37°C. The minimum inhibition zone formed at the edge of the antibiotic disk was calculated. Fig 20 shows the disk diffusion method for MIC calculation. The distance from the antibiotic disk to the inhibition area for every antibiotic was calculated. The one that covered more inhibition zones, i.e., Ciprofloxacin, was selected for a real sample and interference study.

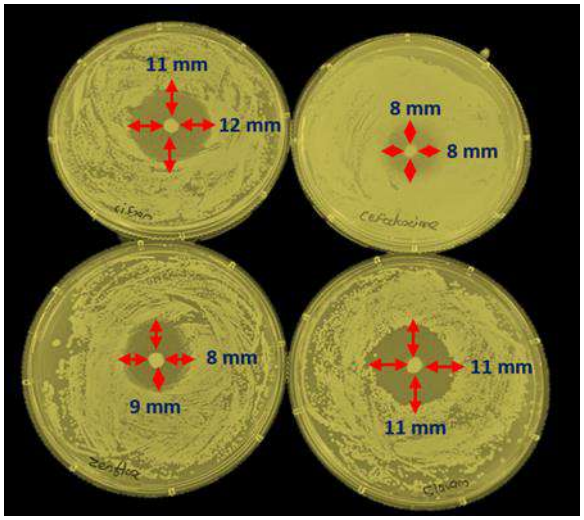

Fig 21. A disk diffusion method for calculation of minimum inhibitory concentration

Multiplexed Electrochemical detection of antibiotic effect over the bacterial growth

The antibiotic susceptibility of E. coli was detected by fabricating a standalone novel multiplexing platform with functionalities of simultaneous culture, detection, on-platform heating, and antimicrobial resistance detection. The device was fabricated by using a 3D printing technique for rapid prototyping. In addition to the functionalities, the developed device has numerous significant. Automation features include a self-powered temperature controller, and step-up and step-down voltage regulators for controlling temperature. Fig 22 illustrates the developed multiplex antibiotic susceptibility testing platform.

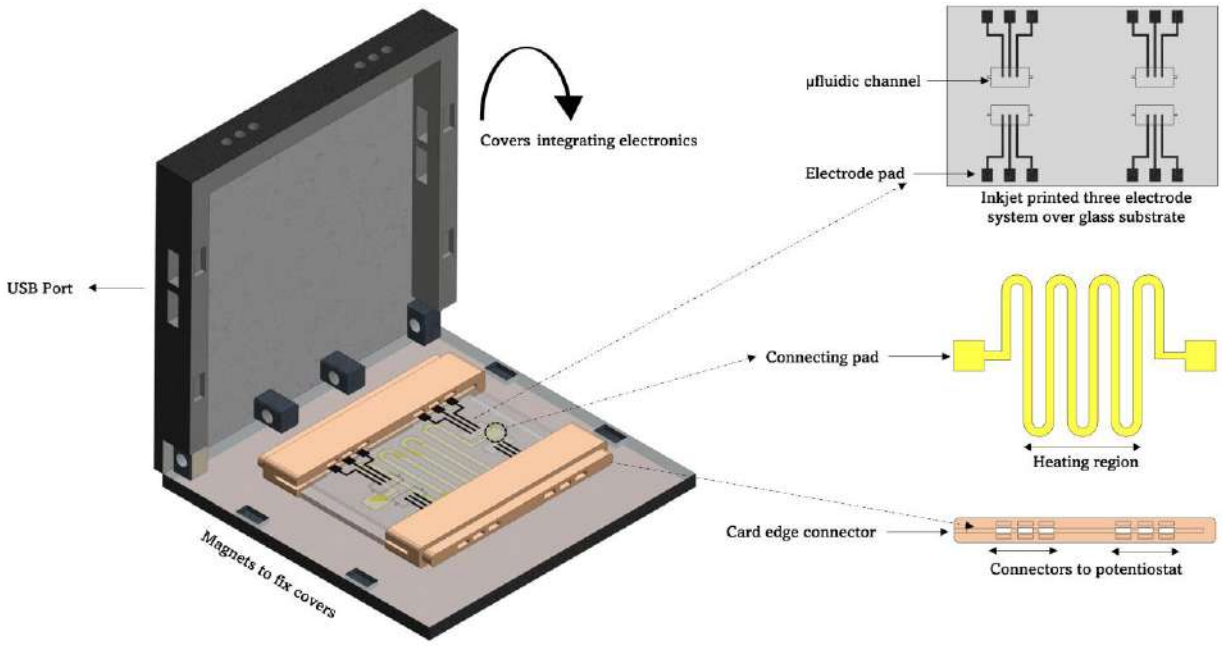

Fig 22. Schematic of developed multiplexed device for bacteria detection and its susceptibility testing

To carry out the electrochemical investigation of bacterial growth inhibition, 100 µg/ml antibiotic concentration of Cefpodoxime, Amoxicillin and Clavulanic acid, Ciprofloxacin, and Ofloxacin with bacteria culture media was injected into four miniaturized reservoirs through the inlet. Before the analysis, the reservoir was washed with 0.1M PBS to prevent cross-contamination. The LIG heater was used to incubate the bacterial culture throughout the experiment, which is necessary for bacterial growth. The electrochemical detection was carried out using CV for 6 hours, and after every hour, the response was recorded. Fig 23 shows the electrochemical reactions of four antibiotics, and their respective calibration plot is given in Fig 24. According to the minimum inhibition zone study, out of four antibiotics, ciprofloxacin was more effective toward E. coli bacterial inhibition. The bacterial concentration would decline in the device with increased time and a constant temperature. In the graph, the current value increases with incubation time because of antibiotics on bacterial growth. The antibiotic helps to increase the transfer of ions in the media, which was blocked by the growth of bacteria.

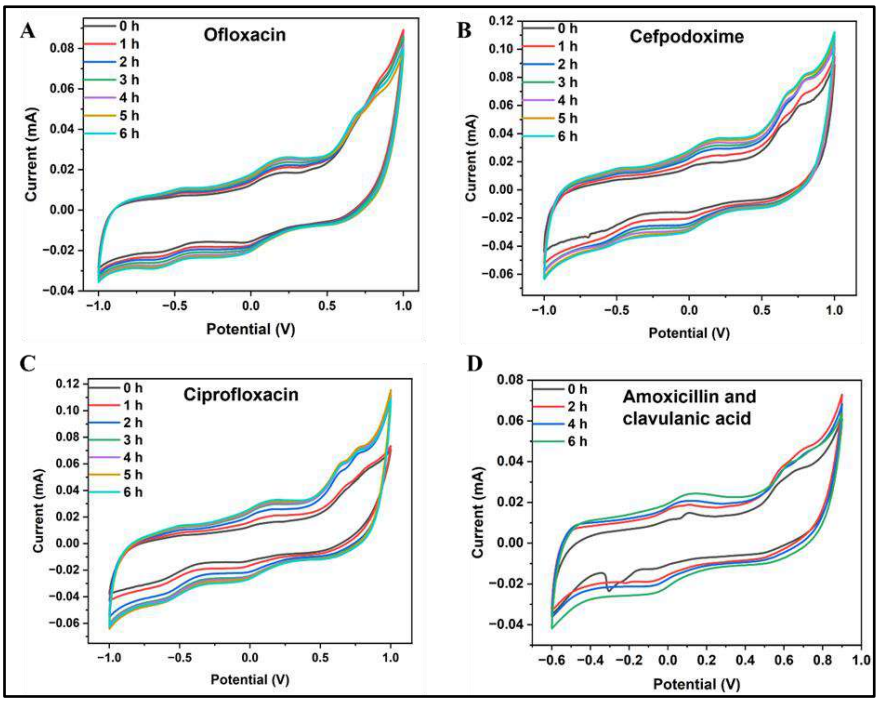

Fig 23. A cyclic voltammetric graph of four antibiotics of 100 µg/ml concentration was performed in the microfluidic device for 6 hours, and the response was recorded at intervals every 1 hour. A) Ofloxacin B) Cefpodoxime C) Ciprofloxacin D) Amoxicillin and clavulanic acid.

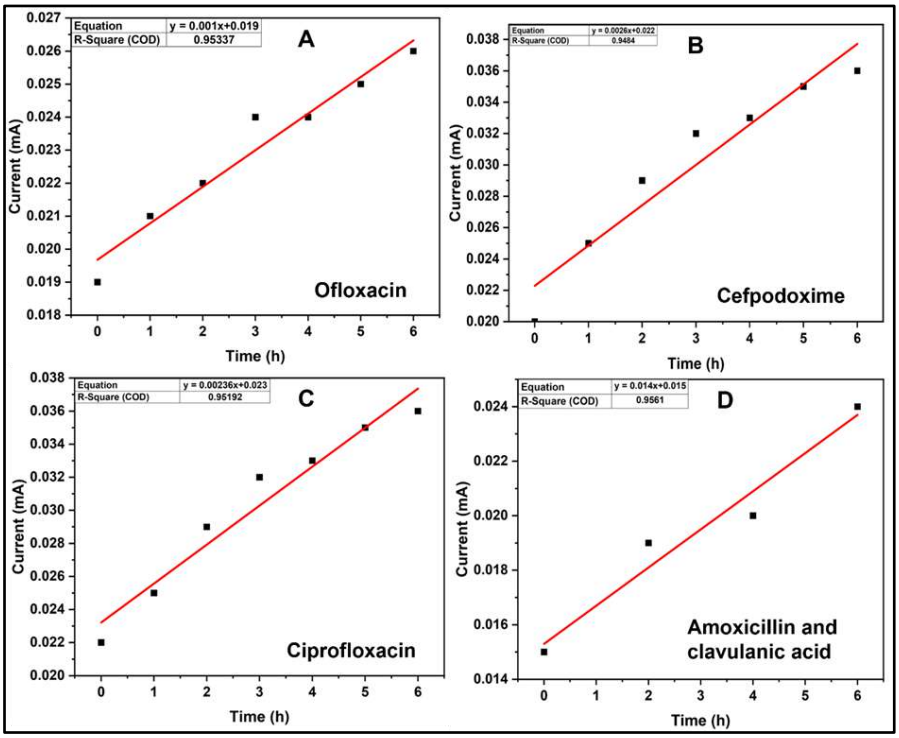

Fig 24 A calibration plot of four antibiotics was performed on the microfluidic device for 6 hours. A) Ofloxacin B) Cefpodoxime C) Ciprofloxacin D) Amoxicilin and clavulinic acid.

Interference study

E. coli and a concentration of the chosen variant's 10^1 CFU mL-1 were used to evaluate several bacterium variants. The device was injected with the same amount of Shewanella putrefaciens and Streptococcus pneumonia, and the resulting peak current responses were compared. The bacteria Shewanella putrefaciens and Streptococcus pneumonia are frequently linked to illnesses and food poisoning. Therefore, these species were chosen to determine the device's selectivity in a real-world situation where these identical bacteria may be present. Streptococcus pneumoniae and Shewanella putrefaciens do not impair the specificity of the E. coli detection, as shown by the corresponding histograms in Fig 25 (A and B) against E. coli and individual variations mixed with E. coli.[49]

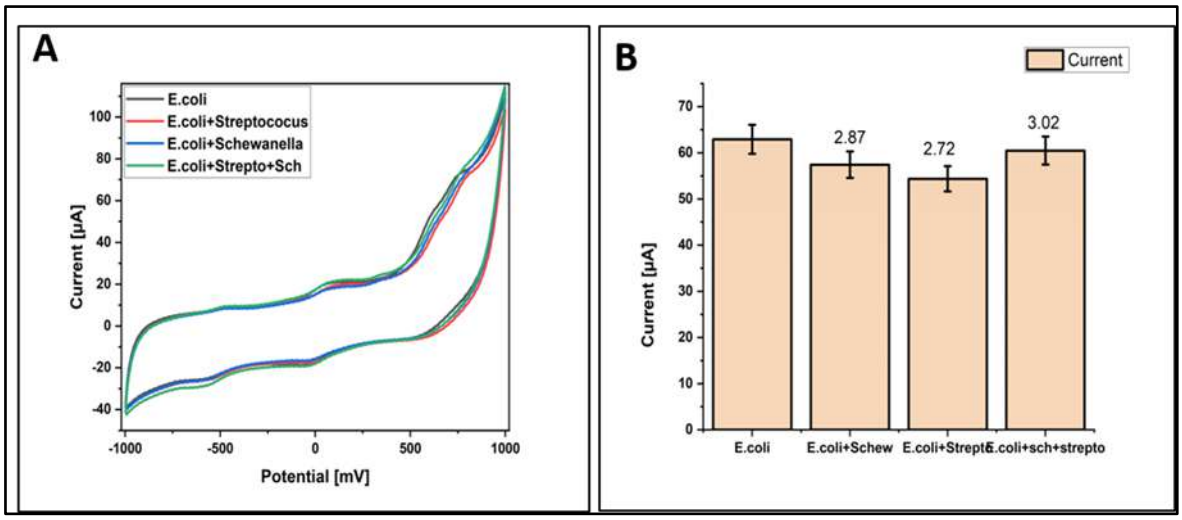

Fig 25**.** Interference study of the electrode with Streptococcus pneumoniae, Shewanella putrefacient (B) The difference in peak current associated with E. coli and the presence of another interferent, Shewanella putrefacient and Streptococcus pneumoniae, are displayed in the histogram.

The specificity of the Clavam antibiotic toward *E. coli* was checked in the developed microfluidic device. The four variants, *Streptococcus, Shewanella, Pseudomonas, and E. coli,* were tested with Clavam antibiotic. The first *E. coli* with Clavam antibiotic was injected into the device, and CV response was recorded. Further, the *pseudomonas, streptococcus, and Shewanella* were added into the same device, and CV response was measured. A similar histogram for *E. coli* and an additional variation of another variant mixed with E. coli is shown in Fig 26. The apparent difference in the inhibition values for *E. coli* and other bacterial species confirms that Ciprofloxacin did not affect *Shewanella Putrefacient, Pseudomonas aeruginosa,*

and Streptococcus Pneumonia.[61] The efficiency of ciprofloxacin against different pathogens was negligible or less than 10%, indicating that it is solely effective against *E. coli* species or that the developed sensor is specific toward *E. coli* species.

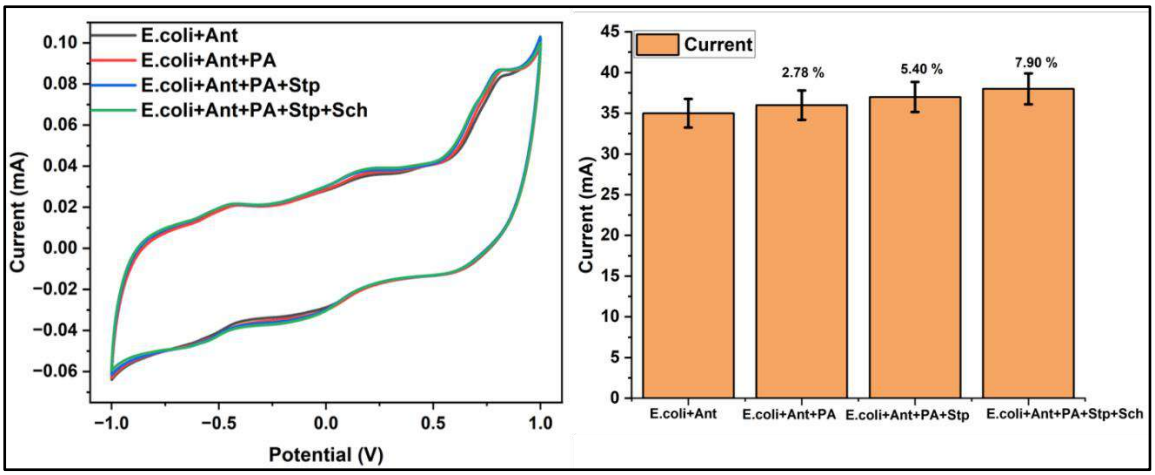

Fig 26. CV graph for specificity study of antibiotics for E. coli, Pseudomonas aeruginosa, streptococcus pneumonia, and *Schewanella putrefacient.*

Real sample analysis

Contagious food microbe E. coli can harm many organs in the human body. The fact that this bacterium can thrive in acidic foods like fruit juices and mayonnaise is challenging for the food manufacturing business. Mango juice was included in the actual sample used for the CV measurement. The signal for mango juice signal acquired at various time intervals is shown in Fig 27 (A&B). The oxidation peak current steadily falls as incubation time goes up. Because the amount of juice decreases, the flow of ions decreases, and the current value decreases as the incubation period lengthens. This confirms the effectiveness of electrochemical detection in foods and drinks.

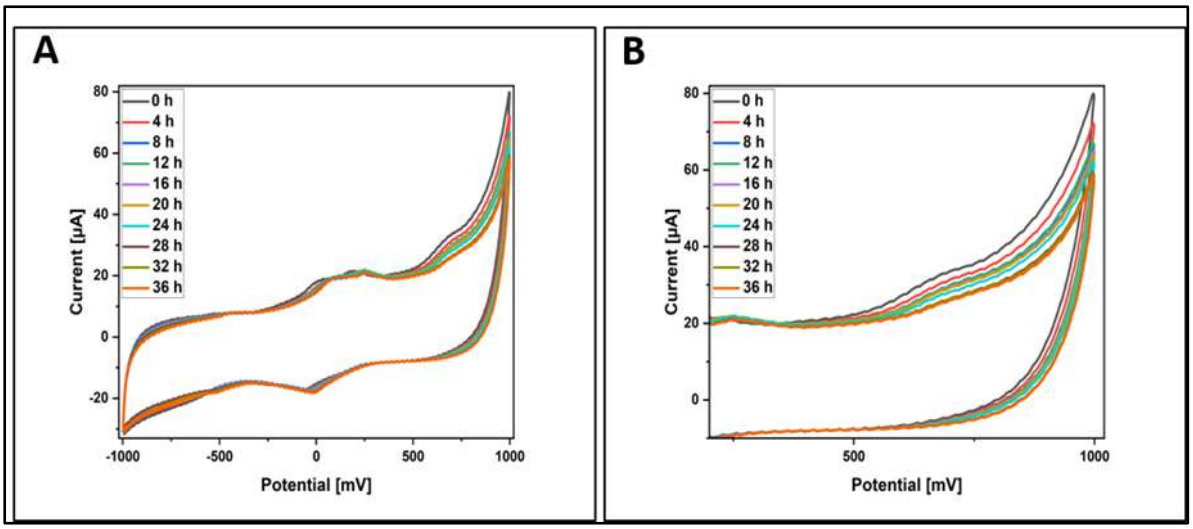

Fig 27 (A) & (B) A microfluidic device captured a cyclic voltammogram for fresh mango juice for 36 hours at four-hour intervals.

A urine sample is mainly used for examining the medical condition. However, obtaining the same quality urine for many illness detections takes time and effort. Hence, synthetic urine was used for experimentation purposes [38]. Along with this, water pollution due to microorganisms is also a significant issue that causes waterborne diseases. Therefore, there was a critical need to detect the microbial pollution of water [39]. Consequently, urine and water samples were selected for accurate sample analysis. Before testing, synthetic urine and tap water were autoclaved to avoid any microbial contamination.

E. coli culture was inoculated into the synthetic urine and tap water before being injected into the device. The electrochemical response was checked for 7 hours at every hour of interval. The CV response of a water sample and synthetic urine is shown in Fig 28. In comparison, without the addition of antibiotic bacterial suspension, the current rise was under the influence of antibiotics [40]. As time increases, the current values also increase because the antibiotic decreases the growth of bacteria. The volume of ions in the urine increases the flow of ions, increasing the current value. This signifies the effect of antibiotics on the growth of bacteria.

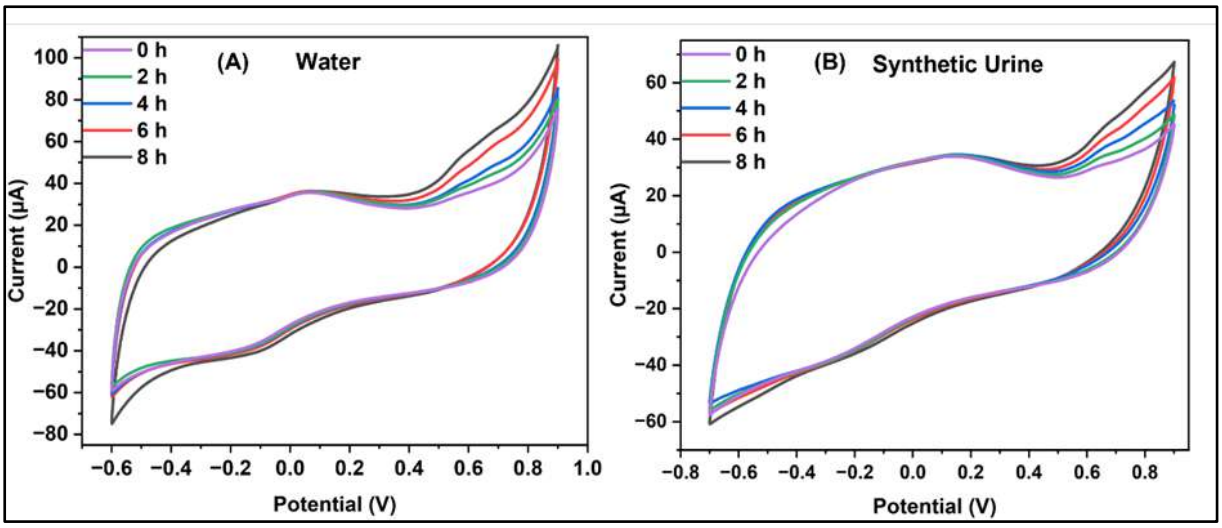

Fig 28. The CV graph for accurate sample analysis performed in the microfluidic device for 7 hours in A) tap water and B) synthetic urine

Impact of the research in the advancement of knowledge or benefit to mankind

Real-time, timely monitoring is the primary method of controlling the spread of antimicrobial resistance. The current approaches to detect bacteria require trained technicians and sophisticated instrumentation and are prone to lengthy experimental turnaround. Over the past decade, the emergence of biosensors for pathogen detection notably developed to counter the limitations of the conventional method.[62]

The testing and rapid detection of pathogenic bacteria are required not only to reduce the mortality of the patients but also to find the resistance developed against multiple drugs in ever-changing bacteria. Therefore, to counter the severe threats exhibited by the pathogenic bacteria, we envisaged a sample-to-answer platform for the rapid, on-site detection of E. coli DH5α and antimicrobial resistance (AMR) strain holds significant potential for public health. By enabling quick and accurate detection of bacterial strains and their resistance patterns directly at the point of need, this platform could revolutionize the management of infectious diseases. It allows for immediate decision-making in clinical settings, reducing the spread of resistant strains and improving patient outcomes.

Additionally, the technology could be deployed in resource-limited environments, enhancing global health efforts by providing a tool that is both accessible and effective. The ability to

rapidly identify AMR in bacteria can help reduce the overuse of antibiotics, thus playing a crucial role in the global fight against antibiotic resistance, one of the most pressing health challenges of our time. This research advances scientific knowledge and offers a tangible benefit to humanity by addressing a critical public health issue.

Literature References

[1] Y. Li, P. Cheng, J. Gong, L. Fang, J. Deng, W. Liang, J. Zheng, Amperometric immunosensor for the detection of Escherichia coli O157:H7 in food specimens, Anal Biochem. 421 (2012) 227–233. https://doi.org/10.1016/j.ab.2011.10.049.

[2] F. Tian, J. Lyu, J. Shi, F. Tan, M. Yang, A polymeric microfluidic device integrated with nanoporous alumina membranes for simultaneous detection of multiple foodborne pathogens, Sens Actuators B Chem. 225 (2016) 312–318. https://doi.org/10.1016/j.snb.2015.11.059.

[3] A. Pandey, Y. Gurbuz, V. Ozguz, J.H. Niazi, A. Qureshi, Graphene-interfaced electrical biosensor for label-free and sensitive detection of foodborne pathogenic E. coli O157:H7, Biosens Bioelectron. 91 (2017) 225–231. https://doi.org/10.1016/j.bios.2016.12.041.

[4] S. Viswanathan, C. Rani, J.A.A. Ho, Electrochemical immunosensor for multiplexed detection of food-borne pathogens using nanocrystal bioconjugates and MWCNT screen-printed electrode, Talanta. 94 (2012) 315–319. https://doi.org/10.1016/j.talanta.2012.03.049.

[5] J. Fernebro, Fighting bacterial infections - Future treatment options, in: Drug Resistance Updates, 2011: pp. 125–139. https://doi.org/10.1016/j.drup.2011.02.001.

[6] J.D. Besant, E.H. Sargent, S.O. Kelley, Rapid electrochemical phenotypic profiling of antibiotic-resistant bacteria, Lab Chip. 15 (2015) 2799–2807. https://doi.org/10.1039/c5lc00375j.

[7] L. Sepunaru, K. Tschulik, C. Batchelor-McAuley, R. Gavish, R.G. Compton, Electrochemical detection of single E. coli bacteria labeled with silver nanoparticles, Biomater Sci. 3 (2015) 816–820. https://doi.org/10.1039/c5bm00114e.

[8] S. Kuss, H.M.A. Amin, R.G. Compton, Electrochemical Detection of Pathogenic Bacteria—Recent Strategies, Advances and Challenges, Chem Asian J. 13 (2018) 2758–2769. https://doi.org/10.1002/asia.201800798.

[9] S. Kuss, H.M.A. Amin, R.G. Compton, Electrochemical Detection of Pathogenic Bacteria—Recent Strategies, Advances and Challenges, Chem Asian J. 13 (2018) 2758–2769. https://doi.org/10.1002/asia.201800798.

[10] Bacterial calibration curve using OD and CFU/ml, 2018. https://www.researchgate.net/publication/323018164.

[11] J. Kang, T. Kim, Y. Tak, J.H. Lee, J. Yoon, Cyclic voltammetry for monitoring bacterial attachment and biofilm formation, Journal of Industrial and Engineering Chemistry. 18 (2012) 800–807. https://doi.org/10.1016/j.jiec.2011.10.002.

[12] H.S. Shin, V. Gedi, J.K. Kim, D. ki Lee, Detection of Gram-negative bacterial outer membrane vesicles using DNA aptamers, Sci Rep. 9 (2019). https://doi.org/10.1038/s41598-019-49755-0.

[13] J.D. Besant, E.H. Sargent, S.O. Kelley, Rapid electrochemical phenotypic profiling of antibiotic-resistant bacteria, Lab Chip. 15 (2015) 2799–2807. https://doi.org/10.1039/c5lc00375j.

[14] H. Zhang, Y. Yao, Y. Hui, L. Zhang, N. Zhou, F. Ju, A 3D-printed microfluidic gradient concentration chip for rapid antibiotic-susceptibility testing, Biodes Manuf. 5 (2022) 210–219. https://doi.org/10.1007/s42242-021-00173-0.

[15] S. Menon, N. Vishnu, S.S.S. Panchapakesan, A.S. Kumar, K. Sankaran, P. Unrau, M.A. Parameswaran, Electrochemical Sensing Methodology for Antibiogram Assays, J Electrochem Soc. 161 (2014) B3061–B3063. https://doi.org/10.1149/2.011402jes.

[16] Y.T. Yang, J.C. Wang, H.S. Chuang, Developing Rapid Antimicrobial Susceptibility Testing for Motile/Non-Motile Bacteria Treated with Antibiotics Covering Five Bactericidal Mechanisms based on Bead-Based Optical Diffusometry, Biosensors (Basel). 10 (2020). https://doi.org/10.3390/BIOS10110181.

[17] Y.T. Yang, J.C. Wang, H.S. Chuang, Developing Rapid Antimicrobial Susceptibility Testing for Motile/Non-Motile Bacteria Treated with Antibiotics Covering Five

Bactericidal Mechanisms based on Bead-Based Optical Diffusometry, Biosensors (Basel). 10 (2020) 1–16. https://doi.org/10.3390/BIOS10110181.

[18] E. Grigorov, S. Peykov, B. Kirov, Novel Microfluidics Device for Rapid Antibiotics Susceptibility Screening, Applied Sciences (Switzerland). 12 (2022). https://doi.org/10.3390/app12042198.

[19] N.J. Cira, J.Y. Ho, M.E. Dueck, D.B. Weibel, A self-loading microfluidic device for determining the minimum inhibitory concentration of antibiotics, Lab Chip. 12 (2012) 1052–1059. https://doi.org/10.1039/c2lc20887c.

[20] S. Smoke, K. Raja, N. Narayanan, L. Brunetti, Selective antibiotic susceptibility reporting and broad-spectrum intravenous antibiotic use: A multicentre ecological study, Int J Antimicrob Agents. 54 (2019) 367–370. https://doi.org/10.1016/j.ijantimicag.2019.06.011.

[21] A.C.M. Veloo, K. Seme, E. Raangs, P. Rurenga, Z. Singadji, G. Wekema-Mulder, A.J. Van Winkelhoff, Antibiotic susceptibility profiles of oral pathogens, Int J Antimicrob Agents. 40 (2012) 450–454. https://doi.org/10.1016/j.ijantimicag.2012.07.004.

[22] H. Jeon, Z.A. Khan, E. Barakat, S. Park, Label-free electrochemical microfluidic chip for the antimicrobial susceptibility testing, Antibiotics. 9 (2020) 1–15. https://doi.org/10.3390/antibiotics9060348.

[23] B. Behera, G.K. Anil Vishnu, S. Chatterjee, V.S.N. Sitaramgupta V, N. Sreekumar, A. Nagabhushan, N. Rajendran, B.H. Prathik, H.J. Pandya, Emerging technologies for antibiotic susceptibility testing, Biosens Bioelectron. 142 (2019). https://doi.org/10.1016/j.bios.2019.111552.

[24] M.A. Hudson, S.W. Lockless, Elucidating the Mechanisms of Action of Antimicrobial Agents, MBio. 13 (2022). https://doi.org/10.1128/mbio.02240-21.

[25] M.A. Hudson, S.W. Lockless, Elucidating the Mechanisms of Action of Antimicrobial Agents, MBio. 13 (2022). https://doi.org/10.1128/mbio.02240-21.

[26] R.A. Ataee, A. Mehrabi-Tavana, S.M.J. Hosseini, K. Moridi, M.G. Zadegan, A method for antibiotic susceptibility testing: Applicable and accurate, Jundishapur J Microbiol. 5 (2012) 341–345. https://doi.org/10.5812/kowsar.20083645.2374.

[27] C. Lee Ventola, The Antibiotic Resistance Crisis Part 1: Causes and Threats, 2015.

[28] T.A. Webster, H.J. Sismaet, I.P.J. Chan, E.D. Goluch, Electrochemically monitoring the antibiotic susceptibility of Pseudomonas aeruginosa biofilms, Analyst. 140 (2015) 7195–7201. https://doi.org/10.1039/c5an01358e.

[29] C.H. Chen, Y. Lu, M.L.Y. Sin, K.E. Mach, D.D. Zhang, V. Gau, J.C. Liao, P.K. Wong, Antimicrobial susceptibility testing using high surface-to-volume ratio microchannels, Anal Chem. 82 (2010) 1012–1019. https://doi.org/10.1021/ac9022764.

[30] T. Pulingam, T. Parumasivam, A.M. Gazzali, A.M. Sulaiman, J.Y. Chee, M. Lakshmanan, C.F. Chin, K. Sudesh, Antimicrobial resistance: Prevalence, economic burden, mechanisms of resistance and strategies to overcome, European Journal of Pharmaceutical Sciences. 170 (2022). https://doi.org/10.1016/j.ejps.2021.106103.

[31] T. Pulingam, T. Parumasivam, A.M. Gazzali, A.M. Sulaiman, J.Y. Chee, M. Lakshmanan, C.F. Chin, K. Sudesh, Antimicrobial resistance: Prevalence, economic burden, mechanisms of resistance and strategies to overcome, European Journal of Pharmaceutical Sciences. 170 (2022) 106103. https://doi.org/10.1016/j.ejps.2021.106103.

[32] A.M. Kaushik, K. Hsieh, L. Chen, D.J. Shin, J.C. Liao, T.H. Wang, Accelerating bacterial growth detection and antimicrobial susceptibility assessment in integrated picoliter droplet platform, Biosens Bioelectron. 97 (2017) 260–266. https://doi.org/10.1016/j.bios.2017.06.006.

[33] K.W. Chang, H.W. Cheng, J. Shiue, J.K. Wang, Y.L. Wang, N.T. Huang, Antibiotic Susceptibility Test with Surface-Enhanced Raman Scattering in a Microfluidic System, Anal Chem. 91 (2019) 10988–10995. https://doi.org/10.1021/acs.analchem.9b01027.

[34] Z.A. Khan, M.F. Siddiqui, S. Park, Progress in antibiotic susceptibility tests: a comparative review with special emphasis on microfluidic methods, Biotechnol Lett. 41 (2019) 221–230. https://doi.org/10.1007/s10529-018-02638-2.

[35] K. Zhang, S. Qin, S. Wu, Y. Liang, J. Li, Microfluidic systems for rapid antibiotic susceptibility tests (ASTs) at the single-cell level, Chem Sci. 11 (2020) 6352–6361. https://doi.org/10.1039/d0sc01353f.

[36] D. Kumar, A.K. Singh, M.R. Ali, Y. Chander, Antimicrobial Susceptibility Profile of Extended Spectrum β-Lactamase (ESBL) Producing Escherichia coli from Various

Clinical Samples , Infectious Diseases: Research and Treatment. 7 (2014) IDRT.S13820. https://doi.org/10.4137/idrt.s13820.

[37] P.C. Tang, O. Eriksson, J. Sjögren, N. Fatsis-Kavalopoulos, J. Kreuger, D.I. Andersson, A Microfluidic Chip for Studies of the Dynamics of Antibiotic Resistance Selection in Bacterial Biofilms, Front Cell Infect Microbiol. 12 (2022) 1–14. https://doi.org/10.3389/fcimb.2022.896149.

[38] H.C. Alves, F. de P.N. Cruz, P.C.P. de Assis, J.D.C. Pessoa, L.C. Trevelin, A.M. de O. Leal, C.P. de Sousa, Antibiotic Resistance among *Escherichia coli*: Isolates and Novel Approaches to the Control of *E. coli* Infections, *Escherichia Coli* - Recent Advances on Physiology, Pathogenesis and Biotechnological Applications. (2017). https://doi.org/10.5772/67400.

[39] S. Hannah, A. Dobrea, P. Lasserre, E.O. Blair, D. Alcorn, P.A. Hoskisson, D.K. Corrigan, Development of a Rapid, Antimicrobial Susceptibility Test for E. coli Based on Low-Cost, Screen-Printed Electrodes, Biosensors (Basel). 10 (2020). https://doi.org/10.3390/bios10110153.

[40] T.A. Duncombe, A.M. Tentori, A.E. Herr, Microfluidics: Reframing biological enquiry, Nat Rev Mol Cell Biol. 16 (2015) 554–567. https://doi.org/10.1038/nrm4041.

[41] Z. Altintas, M. Akgun, G. Kokturk, Y. Uludag, A fully automated microfluidic-based electrochemical sensor for real-time bacteria detection, Biosens Bioelectron. 100 (2018) 541–548. https://doi.org/10.1016/j.bios.2017.09.046.

[42] Z. Altintas, M. Akgun, G. Kokturk, Y. Uludag, A fully automated microfluidic-based electrochemical sensor for real-time bacteria detection, Biosens Bioelectron. 100 (2018) 541–548. https://doi.org/10.1016/j.bios.2017.09.046.

[43] R. Narang, S. Mohammadi, M.M. Ashani, H. Sadabadi, H. Hejazi, M.H. Zarifi, A. Sanati-Nezhad, Sensitive, Real-time and Non-Intrusive Detection of Concentration and Growth of Pathogenic Bacteria using Microfluidic-Microwave Ring Resonator Biosensor, Sci Rep. 8 (2018). https://doi.org/10.1038/s41598-018-34001-w.

[44] R. Narang, S. Mohammadi, M.M. Ashani, H. Sadabadi, H. Hejazi, M.H. Zarifi, A. Sanati-Nezhad, Sensitive, Real-time and Non-Intrusive Detection of Concentration and

Growth of Pathogenic Bacteria using Microfluidic-Microwave Ring Resonator Biosensor, Sci Rep. 8 (2018) 1–10. https://doi.org/10.1038/s41598-018-34001-w.

[45] G.M. Whitesides, The origins and the future of microfluidics, Nature. 442 (2006) 368–373. https://doi.org/10.1038/nature05058.

[46] M. Held, A.P. Lee, C. Edwards, D. V. Nicolau, Microfluidics structures for probing the dynamic behavior of filamentous fungi, Microelectron Eng. 87 (2010) 786–789. https://doi.org/10.1016/j.mee.2009.11.096.

[47] P. Supramaniam, O. Ces, A. Salehi-Reyhani, Microfluidics for artificial life: Techniques for bottom-up synthetic biology, Micromachines (Basel). 10 (2019). https://doi.org/10.3390/mi10050299.

[48] J. Mairhofer, K. Roppert, P. Ertl, Microfluidic systems for pathogen sensing: A review, Sensors (Switzerland). 9 (2009) 4804–4823. https://doi.org/10.3390/s90604804.

[49] S. Fande, K. Amreen, D. Sriram, S. Goel, Microfluidic electrochemical device for real-time culturing and interference-free detection of Escherichia coli, Anal Chim Acta. 1237 (2023). https://doi.org/10.1016/j.aca.2022.340591.

[50] S. Srikanth, U.S. Jayapiriya, S.K. Dubey, A. Javed, S. Goel, A lab-on-chip platform for simultaneous culture and electrochemical detection of bacteria, IScience. 25 (2022). https://doi.org/10.1016/j.isci.2022.105388.

[51] G. Wang, J. Chen, L. Huang, Y. Chen, Y. Li, A laser-induced graphene electrochemical immunosensor for label-free CEA monitoring in serum, Analyst. 146 (2021) 6631–6642. https://doi.org/10.1039/d1an01011e.

[52] S. Fande, S. Srikanth, J. U S, K. Amreen, S.K. Dubey, A. Javed, S. Goel, A protocol to execute a lab-on-chip platform for simultaneous culture and electrochemical detection of bacteria, STAR Protoc. 4 (2023). https://doi.org/10.1016/j.xpro.2023.102327.

[53] M. Rahimnejad, A. Adhami, S. Darvari, A. Zirepour, S.E. Oh, Microbial fuel cell as new technol ogy for bioelectricity generation: A review, Alexandria Engineering Journal. 54 (2015) 745–756. https://doi.org/10.1016/j.aej.2015.03.031.

[54] J. U.S., P. Rewatkar, S. Goel, Miniaturized polymeric enzymatic biofuel cell with integrated microfluidic device and enhanced laser ablated bioelectrodes, Int J Hydrogen Energy. 46 (2021) 3183–3192. https://doi.org/10.1016/j.ijhydene.2020.06.133.

[55] P. Rewatkar, P.K. Enaganti, M. Rishi, S. Mukhopadhyay, S. Goel, Single-step inkjet-printed paper-origami arrayed air-breathing microfluidic microbial fuel cell and its validation, Int J Hydrogen Energy. 46 (2021) 35408–35419. https://doi.org/10.1016/j.ijhydene.2021.08.102.

[56] C. Ding, Y. Liu, Y. Guo, X. Guo, Q. Kang, X. Yan, Z. He, Precise digital bacteria enumeration and antibiotic susceptibility testing via a portable vibrating capillary-based droplet platform, Sens Actuators B Chem. 380 (2023) 133254. https://doi.org/10.1016/j.snb.2022.133254.

[57] J. Karasinski, L. White, Y. Zhang, E. Wang, S. Andreescu, O.A. Sadik, B.K. Lavine, M. Vora, Detection and identification of bacteria using antibiotic susceptibility and a multi-array electrochemical sensor with pattern recognition, Biosens Bioelectron. 22 (2007) 2643–2649. https://doi.org/10.1016/j.bios.2006.10.037.

[58] S. Damiati, U.B. Kompella, S.A. Damiati, R. Kodzius, Microfluidic devices for drug delivery systems and drug screening, Genes (Basel). 9 (2018). https://doi.org/10.3390/genes9020103.

[59] D.S. Wishart, C. Knox, A.C. Guo, S. Shrivastava, M. Hassanali, P. Stothard, Z. Chang, J. Woolsey, DrugBank: a comprehensive resource for in silico drug discovery and exploration., Nucleic Acids Res. 34 (2006). https://doi.org/10.1093/nar/gkj067.

[60] O. Jamieson, T.C.C. Soares, B.A. de Faria, A. Hudson, F. Mecozzi, S.J. Rowley-Neale, C.E. Banks, J. Gruber, K. Novakovic, M. Peeters, R.D. Crapnell, Screen printed electrode-based detection systems for the antibiotic amoxicillin in aqueous samples utilising molecularly imprinted polymers as synthetic receptors, Chemosensors. 8 (2020). https://doi.org/10.3390/chemosensors8010005.

[61] R. Siavash Moakhar, T. Abdelfatah, A. Sanati, M. Jalali, S.E. Flynn, S.S. Mahshid, S. Mahshid, A Nanostructured Gold/Graphene Microfluidic Device for Direct and Plasmonic-Assisted Impedimetric Detection of Bacteria, ACS Appl Mater Interfaces. 12 (2020) 23298–23310. https://doi.org/10.1021/acsami.0c02654.

[62] P. Rao R, S. Sharma, T. Mehrotra, R. Das, R. Kumar, R. Singh, I. Roy, T. Basu, Rapid Electrochemical Monitoring of Bacterial Respiration for Gram-Positive and Gram-Negative Microbes: Potential Application in Antimicrobial Susceptibility Testing, Anal Chem. 92 (2020) 4266–4274. https://doi.org/10.1021/acs.analchem.9b04810.